FLOOD MONITORING USING ERS-1 SAR IMAGERY AND DIGITAL ELEVATION MODEL

Thomas Alexandridis [(1)], Kostas Perakis [(2)], Nikolaos Silleos [(3)]

[(1)] Research Assistant, Aristotelian University of Thessaloniki, Department of Agriculture, Greece, [(2)] Dr., Lecturer in University of Thessaly, Greece, [(3)]Aristotelian University of Thessaloniki, Greece

Abstract: Agricultural crops in plains or depressions (mainly cotton, maize and sugarbeets), suffer not only from diseases and frost, but also from floods, when heavy rains fall during sensitive phenological stages, e.g. during seeding or ripening. The usual cloudy weather, during and after the event, does not allow the use of optical sensors for qualitative and quantitative monitoring of the flooded area. On the other hand, flood monitoring, when images from radar sensors are used, suffer from classification problems, due mainly to the confusion created by the similar radiometric behaviour of flood pixels and the hill shade pixels, resulting in misclassification, qualitatively and quantitatively, of the flood extent and intensity. Digital Elevation Model (DEM) was used to overcome the above difficulties, thus "pushing" the classification algorithm to read only water return signal from plains and depressions and rejecting similar signals from slopping areas.

Keywords: Image analysis, Image Sensors, Satellite applications

1. INTRODUCTION

A disaster flood of agricultural areas occurred in the end of December 1995 and the begin of January1996 in Kilkis prefecture, Macedonia, Greece, mainly along the river Axios and certain flat areas nearby **(Figure 1).**

The Laboratory of Remote Sensing and GIS of the Aristotle University of Thessaloniki was called by the Hellenic Organisation of Agricultural Insurance (HOAI) to propose a methodology for registration of the flooded area, qualitatively and quantitatively, using satellite technology. This method was expected to be more accurate and quick than the traditional field by field (or area by area) estimation conducted by specialist agriculturist. The aims of the study were the accurate delineation of the size of the flooded areas, as well as the flood classification in various intensity classes, that could assist the compensation to the farmers.

1.1. Data sets used

Radar imagery was chosen (ERS-1 SAR) as it was considered ideal for flood monitoring, avoiding the cloud cover that obscured the flooded area, and the low temporal resolution of optical sensors (e.g. Landsat). Large scale topographic maps (1:50,000) from the Hellenic Army Geographical Service were used to overcome the topographic distortion and

accurately register the radar image to a coordinate system. Moreover, elevation contours (20 m interval) were digitised from the topographic maps in order to create a DEM.

1.2 Literature review

Having in mind the side looking nature of the radar, the behaviour of the flooded areas can be explained. Smooth water surfaces act as specular reflectors of radar waves and yield no return to the antenna, but rough water surfaces return radar signals of varying strengths (Lillesand and Kiefer 1993). The major influence, though, is induced by topography. Franklin *et al* (1995), using SEASAT imagery, demonstrate that σ^o (backscattering coefficient) is dependant on topography, a relation that is reduced if the images are radiometrically corrected using a DEM. Parameters related to topography are the terrain slope, aspect and the local angle of incidence of the incoming beam. A simplification of topographically induced radiometric distortions in SAR imagery is an increase in σ^o on slopes facing the radar, and a decrease in σ^o on slopes facing away from the radar. In the same way, slopes having a low incidence angle, give a higher return signal than slopes having a high incidence angle. Bayer et al. (1991) based on SEASAT data concluded that the geometric parameter revealing the strongest influence in σ^o is the local angle of incidence, and suggested a simple correction function based on the calculation of the mean grey value for each incidence angle class. The theoretical basis explaining the possible relationships between radar backscattering coefficient σ^o and soil moisture is well documented. Blyth (1984) showed, using SAR-580 data, that an increase in moisture content, either of soil or vegetation, causes an increase in the electrical conduction properties of the medium (permittivity) which in turn influences the degree of backscattering of microwave radiation, resulting with a brighter return signal. Therefore, it was expected that flood has a low return signal being still water (specular reflection), contrasting with the high response of the surrounding wet soil. In fact the contrast was not so abrupt, implying that flood monitoring is not as simple as an area delineation and need to be explained better.

1.3. Study area

A 17x25 km subset of the total flooded area **(Figure 1)** was used for this study. It is located in the north of Kilkis prefecture, where the river Axios floodplain meets the hilly terrain close to the borders with FYROM (Former Yugoslavia Republic of Macedonia). It was carefully chosen so that to include the man-dried lake Artzan (20 m above sea level), the most severely damaged agricultural area, as well as areas of undulating terrain (350 m above sea level) where the hill shade effect could be confused with water spectral signature. The last was one of the most serious problems which the authors tried to solve using a Digital Elevation Model (DEM) of the survey area. The contours of a topographic map 1:50,000 scale were used to create the DEM.

Figure 1. The location map of the survey area.

2. DATA COLLECTION AND PROCESSING

2.1 Radar imagery

An ERS-1 SAR full scene was ordered (100x100 km, 12.5 pixel size, 25 m resolution (December 30, 1995 acquisition date), and processed in Matera, Italy. A subset (**Figure 2**) was extracted that included the study area and was processed for speckle suppression. This would not only clear the image of unreal values

Figure 2. The subset of the Radar image used

and give a better visual appearance, but also force spectral features to better approximate the normal distribution (Trevett 1986, Dobson *et al* 1995). The Lee-sigma filter was applied twice so that the "salt and pepper" appearance of the image improved with as less as possible impact on the spatial resolution. According to Blyth (1984) accurate radiometric calibration and across track balancing is required for the radar images to enable the derivation of backscattering coefficient σ^o. The image was calibrated to σ^o values using the formulae presented in Laur (1992). These take into account the earth curvature and radar local depression angle. The image was provided in CEOS format and all the information needed were found in the file headers. Subsequently the image was geometrically corrected using 16 ground control points (GCP's) evenly distributed around the study area. 1:50,000 scale maps were used to measure the GCP's coordinates. Their location on the image was proven to be much more difficult to identify than expected, due to the lack of easy-to-identify features (cross-roads, bridges) on the hilly part of the study area. A second order transformation was chosen as it provided better results in the undulating terrain around the floodplain. The rms error was calculated to be 2.61 pixels (x: 1.91, y: 1.68), which is acceptable according to Leberl (1990). The rms x coordinate is much bigger due to the inherent distortion in the radar range direction. At the end, the image was registered to the Universal Transverse Mercator coordinate system (UTM), resampled to 20 m pixel size with the nearest neighbour algorithm, so that the original values were preserved.

2.2 Digital Elevation Model (DEM)

Elevation contours (20 m interval) and spot heights were digitised from the topographic maps to create a DEM (**Figure 3**).

Figure 3. The Digital Elevation Model

The contour coverage was slightly larger than the extents of the study area, to ensure that no edge information would be lost. From the elevation data and using the Arc/Info (ESRI Inc. 1996) routines a 20 m spacing elevation grid was created (**Figure 2**). The interpolation method is specifically designed for the creation of hydrological correct DEMs. It is based upon the ANUDEM program developed by Hutchinson (Hutchinson 1988, 1989), designed to have the computational efficiency of 'local' interpolation methods, such as inverse distance weighted interpolation, without losing the surface continuity of global interpolation methods such as kriging and splines (ESRI Inc. 1994). Furthermore, a contour coverage was created from the DEM and was compared to the digitised one, in order to check for any errors induced by the algorithm. Using the Arc/Grid (ESRI Inc. 1996) routines and the DEM, a percentage slope grid was created. The slopes in the study area range from 0 to 65 %. The ERS-1 SAR image was fused together with the elevation grid and the slope grid as a single 3-layer image, in order to exploit better the information of the combined layers (Pertrie *et al* 1994).

2.3 Ground data

The flood area was visited on January 5, 1996. Due to restraints of time and equipment (GPS), no detailed field data were collected. Only the area of the ex-lake Artzan was identified as being completely covered with deep water (50-60 cm). Another area was also identified on the map as being completely intact by the flood, and moreover there was no claim by the farmers for damage compensation **(Figure 4**).

Figure 4. The flooded area.

3. FLOOD EXTENT AND INTENSITY DETERMINATION

First step is to define the meaning of intensity classes that could be detected by radar imagery. Having visited the flooded area, it appeared that parts, completely covered by water, gave way to intact parts gradually due to the lack of topography. That is, moving away from the 100% flooded areas, small "islands" appeared and the percentage of land emerging from flood water, increased until the water was restricted in small ponds. Having in mind the nature of the radar waves, it is evident that the flood/land percentage is recorded by the satellite image and not the flood intensity (i.e. flood depth). Indeed, the radar return signal increases gradually with the increase of the emerging land percentage, since the target stops acting as a specular reflector being rougher. Land surface roughness is a major factor that controls the radar return signal (Alexandridis 1996), and it is the feature that explains more of the variance in C band (Evans 1984). Sample points from various area features were extracted from the 3-layer image. The samples were area based and not pixel based in order to avoid erroneous results imported by the inherent speckle of the image.

The sampled features include:

- 100% flood, identified in the ex-lake Artzan
- 0% flood, sampled in various locations in order to cover the image radiometry of all the features existing in the level terrain except the flood
- area in a slope of a hill facing the radar in a slope of a hill facing away from radar (hill shade)

In order to understand better the behaviour of these features in the radar image and to assist the classification algorithm, the samples were plot as a feature space image (**Figure 5**). It is evident in **Figure 5** that the radar image only, would not be adequate to discriminate between flood and hill shade. On the other hand, by using the other layers of the image, a simple box classification algorithm would be able to delineate correctly the flood pixels from the other features of the image.

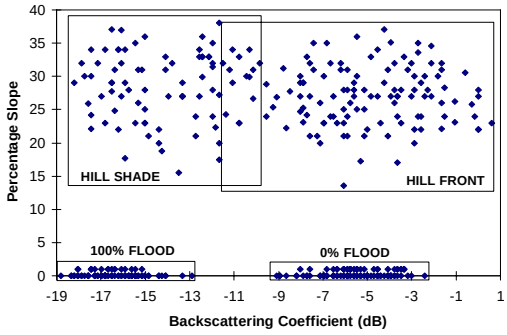

Figure 5. Feature space image of σ^o against percentage slope using sample areas. The boxes were plot based on the ±3 standard deviations from the sample means.

3.1 Normality tests

After converting the 16-bit image to 8-bit (0-255) in order to reduce the extended range of the distribution of the values of flood sample, normality is examined by calculations of the mean, the 5% trimmed mean and the median of the distribution. The 5% trimmed mean $T_{0,9}$ is:

$$T_{0,9} = \frac{1}{0{,}9\sum_{k=1}^{m} c_k}\left[\left(\sum_{k=1}^{k_1+1} c_k - 0{,}05\sum_{k=1}^{m} c_k\right) y_{k_1} + \left(\sum_{k=1}^{m} c_k + \sum_{k=1}^{k_2-1} c_k - 0{,}05\sum_{k=1}^{m} c_k\right) y_{k_2} + \sum_{i=k_1+2}^{k_2-1} c_i y_i\right]$$

where $y_1<...<y_m$, are m ordered observations for the sample and $c_1,...,c_m$ are the corresponding case-weights and

$$\sum_{k=1}^{k_1} c_k < 0{,}05\sum_{k=1}^{m} c_k < \sum_{k=1}^{k_1+1} c_k \text{ and}$$

$$\sum_{k=1}^{m} c_k - \sum_{k=1}^{k_2} c_k < 0{,}05\sum_{k=1}^{m} c_k$$

$$..... < \sum_{k=1}^{m} c_k - \sum_{k=1}^{k_2-1} c_k \quad [1]$$

Tabulating the results for the trimmed means above and calculating the Adrews et al (1996) M-estimators, corresponding to the two chosen samples of flood and dry land area, separately, we observe that there are not markedly different values neither in the case of the trimmed means nor in the case of the M-estimators. As a result, we have distributions that are symmetric, smooth, continuous with tails similar to those of the normal distribution and therefore we consider that we are close to normality (Hoaglin et al, 1983).

3.2 Classification method

Once the normality of the various samples were checked, 5% from the data of each feature were excluded as outliers (speckle) in order to identify the radiometric extents of the flood in the feature space image. The flood radiometric range was divided in 6 flood intensity classes (**Table 1**), but the results are presented in one class for easier evaluation by the HOAI decision makers **(Figure 4).** The box classification algorithm was employed within a model created in ERDAS Imagine v8.2 (ERDAS Inc., 1996). The results are presented in **Table 2**, while a perspective view of the flooded area is displayed in **Figure 4.**

4. RESULTS AND DISCUSSION

A simple and operational method of flood monitoring is presented. An ERS-1 SAR image was processed for speckle suppression, calibrated to σ^o values and georeferenced to UTM coordinate system. Elevation contours from 1:50,000 topographic maps were digitised and a digital elevation model (DEM) was created, as well as a percentage slope raster layer. The major difficulty encountered was the separation of the flood pixels from the hill shade pixels, due to the similar radiometric behaviour in radar images. It was overcome with the implementation of the DEM and the fusion of the topographic information with the radar image. Indeed, slope and elevation was the discriminate factor as flood appeared in low elevation and in minimum slope. Using minimum amount of ground data the flooded area can be divided in 6 classes of flood intensity, having the normality of the samples tested with robust estimators. The results confirm the gravity of the damage in the area, being mainly agricultural, with a total area of 1669.6 hectares flooded on December 30, 1995. The results of the study are also of use to other public organisations and local authorities, in order to assist the clean-up effort and improve the flood control systems.

Unfortunately the limited ground data restricted the detailed interpretation of the classification results, especially the meaning and the importance of intensity classes. Future work should concentrate on detailed ground data collection. A time series of radar images would enable the monitoring of the flood track. With

Table 1 - Radiometric ranges of flood intensity classes

Class	Percentage of flood	Range of σ^o (dB)
1	0-20	-8.941 -9.698
2	21-40	-9.699 -10.456
3	41-60	-10.457 -11.214
4	61-80	-11.215 -11.973
5	81-99	-11.974 -12.731
6	100	-12.732 -20.011

Table 1. Radiometric ranges of flood intensity classes.

Table 2 - Flood extent results

Class	Percentage of flood	Flood extent (ha)
1	0-20	568.2
2	21-40	401.2
3	41-60	258.5
4	61-80	157.8
5	81-99	113.9
6	100	170.0
	Total	**1669.6**

Table 2. Flood extent results

the use of cadastral maps (a work expected to be completed the next decade in Greece, but products are already used gradually), the time that each cultivated field is kept under water could be estimated. Therefore, the compensation to each farmer would be calculated quicker and more accurate than using the present methods.

REFERENCES

Alexandridis, T., (1996). Terrain and soil influences on ERS-1 SAR images. *MSc Thesis, Silsoe College Library, Cranfield University.*

Andrews, D.F., Bickel, P.J., Hampel, F.R., Huber, P.J., Rogers, W.H. , and Tukey, .W. (1972*). In Robust Estimates of Location:Survey and Advances. Princeton, NJ*: (Princeton University Press).

Bayer, T., Winter, R. and Schreier, G., 1991, Terrain influences in SAR backscatter and attempts to their correction. *In Transactions in Geoscience and Remote Sensing*, vol.29, No.3, pp.451-462

Blyth, K., (1984). Analysis of digital radar data from SAR-580 data in relation to soil-vegetation moisture and roughness. *In Proceedings of the SAR-580 investigators workshop* (Ispra:Joint Research Centre and ESA, Italy).

Dobson, M.C., Ulaby, F.W. and Pierce, L.E., (1995). Land-cover classification and estimation terrain attributes using synthetic aperture radar. In *Remote Sensing of Environment*, 51:199-214.

Environmental Systems Research Institute, Inc, 1994, *ARC Commands*. (ESRI Inc., New York).

Evans, R., (1984). Synthetic aperture radar imagery for soil survey in lowland England. In *Proceedings of the SAR-580 investigators workshop* (Ispra: Joint Research Centre and ESA, Italy).

Franklin, S.E, Lavigne, M.B, Hunt, E.R.Jr, Wilson, B.A, Peddle, D.R, McDermid, G.J. and Giles, P.T., (1995). Topographic dependence of Synthetic Aperture Radar imagery. In *Computers and Geosciences*, vol.21, No. 4, pp. 521-532

Hoaglin, D.C., Mosteller F., Tukey J.W. (1983*). In Undarstanding robust and exploratory data analysis*, (John Wiley & Sons, Inc.).

Hutchinson, M.F., (1988). Calculation of hydrologically sound digital elevation models. In *Third International Sysmposium on Spatial Data Handling, Sydney* (Columbus, Ohio: International Geographical Union).

Hutchinson, M.F., (1989). A new procedure for gridding elevation and stream line data with automatic removal of spurious pits. In *Journal of Hydrology*: 106, 211-232.

Petrie, G.M., Wukelic, G.E., and Kimball, C.S., (1994). *Responsiveness of satellite remote sensing and image processing technologies for monitoring and evaluating 1993 Mississippi river flood developments using ERS-1 SAR* (Landsat, and SPOT digital data. ASPRS/ACSM ,1994).

Laur, H., (1992). Derivation of backscattering coefficient σ^o in ERS-1.SAR.PRI products. *In European Space Agency Bulletin, Issue 1, Rev.0*

Leberl, F.W., (1990). *Radargrammetric image processing* (Artech House, Inc.).

Liliesand, T.M and Kiefer, R.W., 1993, *Remote sensing and image interpretation.* (John Willey and Sons Inc. Third Edition).

Trevett, J.W., (1986). *Imaging radar for resources surveys*. In Chapman and Hall.